*Human Molecular Genetics*, 2016, Vol. 25, No. 14 2948–2958

**doi: 10.1093/hmg/ddw146**
Advance Access Publication Date: 14 May 2016
Original Article

ORIGINAL ARTICLE

# BIN1 regulates BACE1 intracellular trafficking and amyloid-β production

Toji Miyagawa[1,2], Ihori Ebinuma[1], Yuichi Morohashi[1], Yukiko Hori[1], Mee Young Chang[3], Haruhiko Hattori[4], Tomoaki Maehara[4], Satoshi Yokoshima[4], Tohru Fukuyama[4], Shoji Tsuji[2], Takeshi Iwatsubo[5], George C. Prendergast[3] and Taisuke Tomita[1,*]

[1]Laboratory of Neuropathology and Neuroscience, Graduate School of Pharmaceutical Sciences, [2]Department of Neurology, Graduate School of Medicine, The University of Tokyo, 113-0033 Japan, [3]Lankenau Institute for Medical Research, PA 19096, USA, [4]Laboratory of Natural Products Chemistry, Graduate School of Pharmaceutical Sciences, Nagoya University, 464-8601 Japan and [5]Department of Neuropathology, Graduate School of Medicine, The University of Tokyo, 113-0033 Japan

*To whom correspondence should be addressed at: Laboratory of Neuropathology and Neuroscience, Graduate School of Pharmaceutical Sciences, The University of Tokyo, 7-3-1 Hongo, Bunkyo-ku, Tokyo 113-0033, Japan. Tel: +81-3-5841-4868; Fax: +81-3-5841-4708; Email: taisuke@mol.f.u-tokyo.ac.jp



## Abstract

*BIN1* is a genetic risk factor of late-onset Alzheimer disease (AD), which was identified in multiple genome-wide association studies. BIN1 is a member of the amphiphysin family of proteins, and contains N-terminal Bin-Amphiphysin-Rvs and C-terminal Src homology 3 domains. BIN1 is widely expressed in the mouse and human brains, and has been reported to function in the endocytosis and the endosomal sorting of membrane proteins. BACE1 is a type 1 transmembrane aspartyl protease expressed predominantly in neurons of the brain and responsible for the production of amyloid-β peptide (Aβ). Here we report that the depletion of BIN1 increases cellular BACE1 levels through impaired endosomal trafficking and reduces BACE1 lysosomal degradation, resulting in increased Aβ production. Our findings provide a mechanistic role of BIN1 in the pathogenesis of AD as a novel genetic regulator of BACE1 levels and Aβ production.

## Introduction

Alzheimer disease (AD) is the leading cause of dementia worldwide. Several lines of evidence suggested that the deposition of amyloid-β peptide (Aβ) in the brain is the essential pathological trigger of AD. Aβ is generated from amyloid-β precursor protein (APP) through its sequential proteolytic cleavages by β- and γ-secretases. Different groups independently identified a membrane-spanning aspartic protease, now called β-site APP-cleaving enzyme 1 (BACE1), as the β-secretase (1–5). BACE1 is a 501 amino acid N-glycosylated type 1 transmembrane aspartyl protease that is expressed predominantly in neurons of the brain. BACE1 cleaves APP to release a soluble ectodomain known as sAPPβ, as well as the membrane-bound stub C99, which is cleaved by γ-secretase to produce Aβ. BACE1 mainly localizes at the *trans*-Golgi network and endosomes by an ADP-ribosylation factor 6 (Arf6)-mediated non-clathrin dependent endocytic pathway (6,7). Optimal enzyme activity of BACE is achieved in acidic pH, and the cleavage of APP by BACE1 occurs mainly in the Rab5 positive early endosomes, which have an acidic intracellular environment. Thus, the endocytosis and

**Received:** April 13, 2016. **Revised:** April 13, 2016. **Accepted:** May 9, 2016

membrane trafficking of APP and secretases are crucial for Aβ production (8).

The *bridging integrator 1* (*BIN1*) gene was identified as a genetic risk factor of late-onset AD by the genome-wide association studies (9). A large two-stage meta-analysis of 74 046 individuals found that having the minor allele (T) at rs6733839, which locates at 27.1 kb upstream from *BIN1* coding locus, is a genetic risk for AD, with an odds ratio of 1.18–1.25 and a minor allele frequency of 0.409 (10). BIN1 is a member of the amphiphysin family proteins, which contains an N-terminal Bin-Amphiphysin-Rvs (BAR) and C-terminal Src homology 3 (SH3) domains, which are implicated in the membrane bending/tubulation and dynamin recruitment, respectively (11). BIN1 was originally identified as a protein that is required for T-tubule formation in muscle tissue (12,13). However, BIN1 is ubiquitously expressed in the central nervous system (CNS) and other organs as multiple isoforms. CNS-specific isoforms 1–7 contain a clathrin and AP-2 adaptor complex binding (CLAP) domain (14), which are involved in the clathrin-mediated endocytosis from the cell surface. In addition, BIN1 plays important roles in intracellular endosomal vesicle sorting (15,16). These data suggest that BIN1 affects the molecular pathobiology of AD by regulating the membrane trafficking of AD associated proteins. BIN1 expression correlates with neurofibrillary tangle pathology and is implicated in tau pathology (17). However, pathological effect of BIN1 on APP metabolism still remains unclear. In this study, we found that BIN1 regulates Aβ production through modulation of the lysosomal targeting of BACE1, suggesting the possibility that BIN1 affects AD risk by modulation of the intracellular trafficking of BACE1.

## Results

### Reduced level of BIN1 increased A$\beta$ secretion and cellular BACE1 level

*Bin1* knockout mice are perinatal lethal because of cardiomyopathy (18). Thus we obtained primary cortical neurons from the brains of postnatal day (P) 1 pups of $Bin1^{flox/flox}$ mice (19), and infected them with recombinant lentiviruses encoding Cre recombinase to deplete the expression of *Bin1* in neurons. Immunoblot analysis of cell lysates demonstrated that BACE1 expression levels were significantly increased in Cre-expressing $Bin1^{flox/flox}$ neurons (Fig. 1A). In contrast, the expression levels of the APP holoprotein and nicastrin, which is a component of the γ-secretase, were not altered. Consistent with the increased levels of BACE1, sAPPβ secretion in the conditioned medium was significantly increased in Cre-expressing $Bin1^{flox/flox}$ neurons without affecting sAPPα level. Moreover, we found higher levels of Aβ40 and Aβ42 in the medium of Cre-expressing $Bin1^{flox/flox}$ neurons than in the medium of neurons infected with control lentivirus (Fig. 1B). The proportion of Aβ42 to total Aβ (sum of Aβ40 and Aβ42) was not altered by *Bin1* depletion (Fig. 1C). These data indicated that β-secretase activity was enhanced by the ablation of *Bin1* expression. Alternative splicing of *Bin1* mRNA results in the production of several isoforms of BIN1, including CLAP domain-containing neuron specific isoform (11,14,20,21), implicating the cell type-specific function of BIN1. However, we confirmed the increased secretion of Aβ and cellular BACE1 levels by RNAi knockdown against *Bin1*, not only in mouse neuroblastoma Neuro2a cells (Fig. 2A and B), but in human non-neuronal HeLa cells (Fig. 2D and E), suggesting that the general function of BIN1 is involved in the modulation of β-secretase activity. To assess whether enzymatically active BACE1 was increased by *Bin1* depletion, BACE1 activity in the membrane fractions of Neuro2a cells was analyzed by an *in vitro* assay using the recombinant substrate JMV2236 (22). *Bin1* RNAi in Neuro2a cells significantly increased the BACE1 activity in the membrane fraction, indicating that increased cellular BACE1 levels by *Bin1* depletion correlated with enhanced BACE1 activity, thereby increasing Aβ production (Fig. 2C). Furthermore, we did not observe any change in Aβ secretion from *Bin1*-ablated HeLa cells expressing APP C99, which is a direct substrate of γ-secretase (Supplemental Material Figure S1). These results clearly indicated that the increased Aβ secretion from *Bin1*-depleted cells was due to enhanced β-cleavage by BACE1.

### BIN1 regulates the intracellular trafficking of BACE1

In addition to endocytosis and membrane recycling, BIN1 has been implicated in cytoskeleton regulation, DNA repair, cell cycle progression, and apoptosis (9,11,23). To investigate the mechanism as to how BIN1 regulates cellular BACE1 levels, we first examined the mRNA levels of BACE1 in Cre-expressing $Bin1^{flox/flox}$ neurons. Although cellular BACE1 protein levels were increased, mRNA levels of BACE1 were not altered in Cre-expressing $Bin1^{flox/flox}$ neurons ($99.8 \pm 0.5\%$ compared with control neurons, $n = 6$). We next tested the effect of BIN1 on the trafficking of BACE1. Immunofluorescence staining of BIN1 in HeLa cells showed a diffuse cytosolic distribution that was diminished by *Bin1* RNAi, as described previously in (data not shown) (14). Notably, BACE1 staining was enhanced predominantly in the perinuclear compartment of *Bin1*-depleted cells, and merged with EEA1-positive early endosomes (Fig. 3A). Intriguingly, EEA1 positive early endosomes were enlarged in the *Bin1* depleted cells, suggesting that BIN1 regulates endocytosis from the cell surface and/or the intracellular trafficking of endocytic vesicles containing BACE1. To evaluate the endocytosis and trafficking of BACE1 from the plasma membrane, we utilized SNAP tag technology to specifically visualize cell surface BACE1 (SNAP-BACE1) (24,25) (Fig. 3B). SNAP tag is a 20 kDa mutant of $O^6$-alkylguanine-DNA alkyltransferase that reacts specifically and rapidly with benzylguanine derivatives, leading to irreversible covalent labeling of the SNAP tag with a synthetic probe. In this assay, SNAP-Surface Alexa Fluor 488, cell impermeable fluorescent substrate, selectively labels N-terminally SNAP-tagged BACE1 on the cell surface. Thirty minutes after labeling, labeled SNAP-BACE1 was internalized and accumulated in the EEA1-positive early endosomes without an apparent difference between in the *Bin1*-depleted cells and the control cells (Fig. 3C). However, 120 min after labeling, a large fraction of the labeled SNAP-BACE1 had disappeared from the EEA1-positive early endosomes in the control cells (Fig. 3C). Intriguingly, in the *Bin1*-depleted cells, the majority of labeled SNAP-tagged BACE1 still remained in the EEA1-positive early endosomes, suggesting that BIN1 functions in the intracellular trafficking of BACE1 from the early endosomes.

The accumulation of BACE1 might be due to the impaired trafficking of BACE1 to late endosomes/lysosomes or a defect in its recycling to the cell surface. We next analyzed the BACE1 degradation, in which the lysosomal pathway is involved (26–28). We performed subcellular fractionation using sucrose density gradients using Neuro2a cells. LAMP1, GM130, transferrin receptor (TfR), and EEA1 were used as markers for late endosomes/lysosomes, the Golgi complex, recycling endosomes, and early endosomes, respectively. We found that LAMP1 was

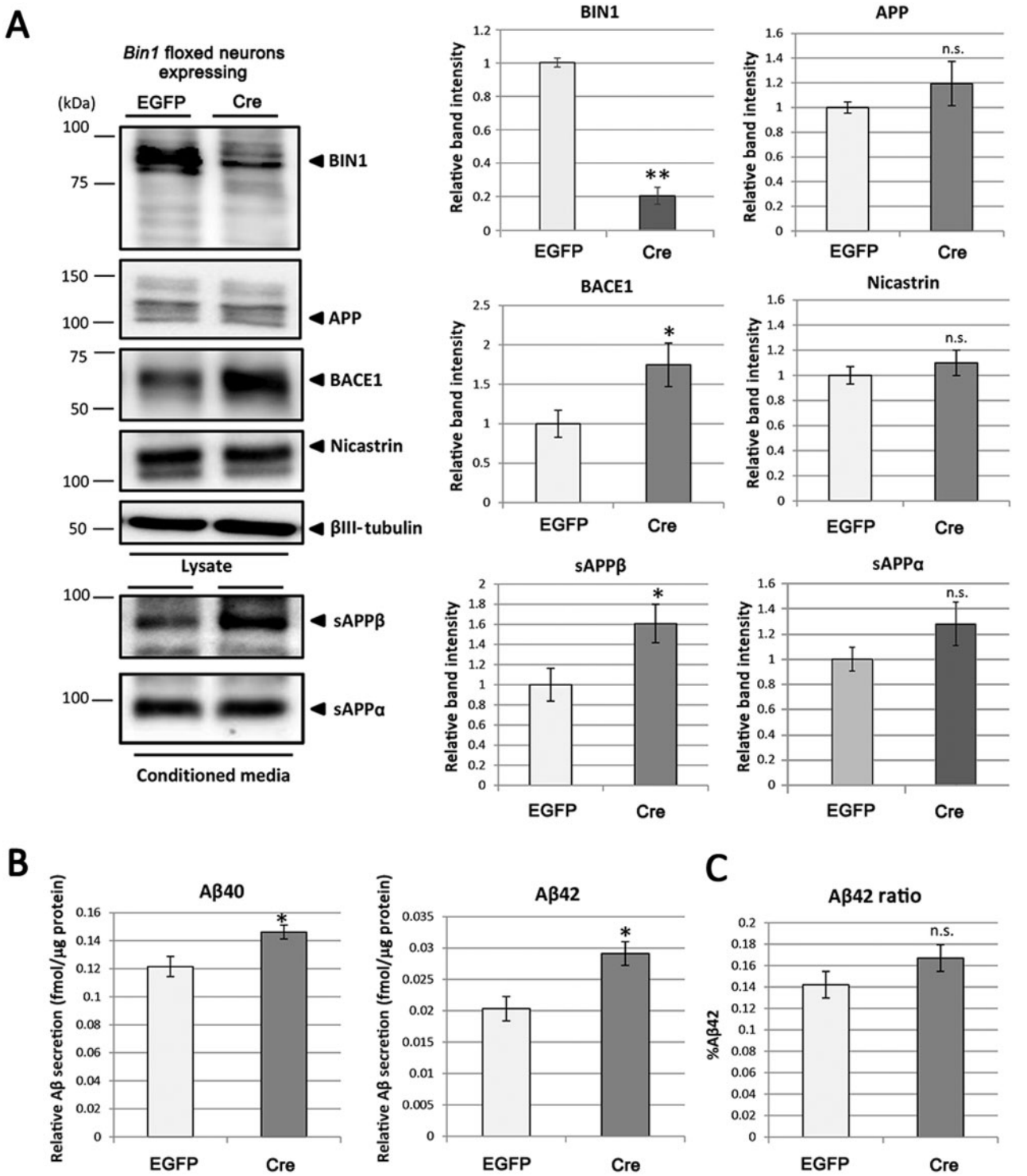


**Figure 1.** Depletion of BIN1 increased A$\beta$ secretion and BACE1 levels in primary neurons. (**A**) Primary cortical neuron cultures from *Bin1*$^{flox/flox}$ mice infected either with either EGFP-NLS (EGFP) or EGFP-NLS-Cre (Cre) expressing lentiviruses were analyzed by immunoblotting. Relative band intensities are indicated at the right ($n = 6$, mean± SEM, *$P < 0.05$). (**B**) Levels of A$\beta$40 and A$\beta$42 secreted from primary cortical neuron cultures were quantitated by sandwich ELISAs ($n = 6$, mean± SEM, *$P < 0.05$). (**C**) Percentages of A$\beta$42 as a fraction of total A$\beta$ (sum of A$\beta$40 and A$\beta$42) in the experiment (B) ($n = 6$, mean ± SEM, *$P < 0.05$).

detected predominantly in the low density fraction (fraction 2), whereas other organelle markers were detected diffusely in the high-density fraction (Fig. 4A). In the *Bin1*-depleted cells, BACE1 in the fraction 2, which corresponds to late endosomes/lysosomes, was significantly reduced compared with the control cells (Fig. 4B). These results indicated that the intracellular trafficking of BACE1 from the early endosomes to the lysosomal pathway was impaired in the *Bin1* depleted cells, resulting in

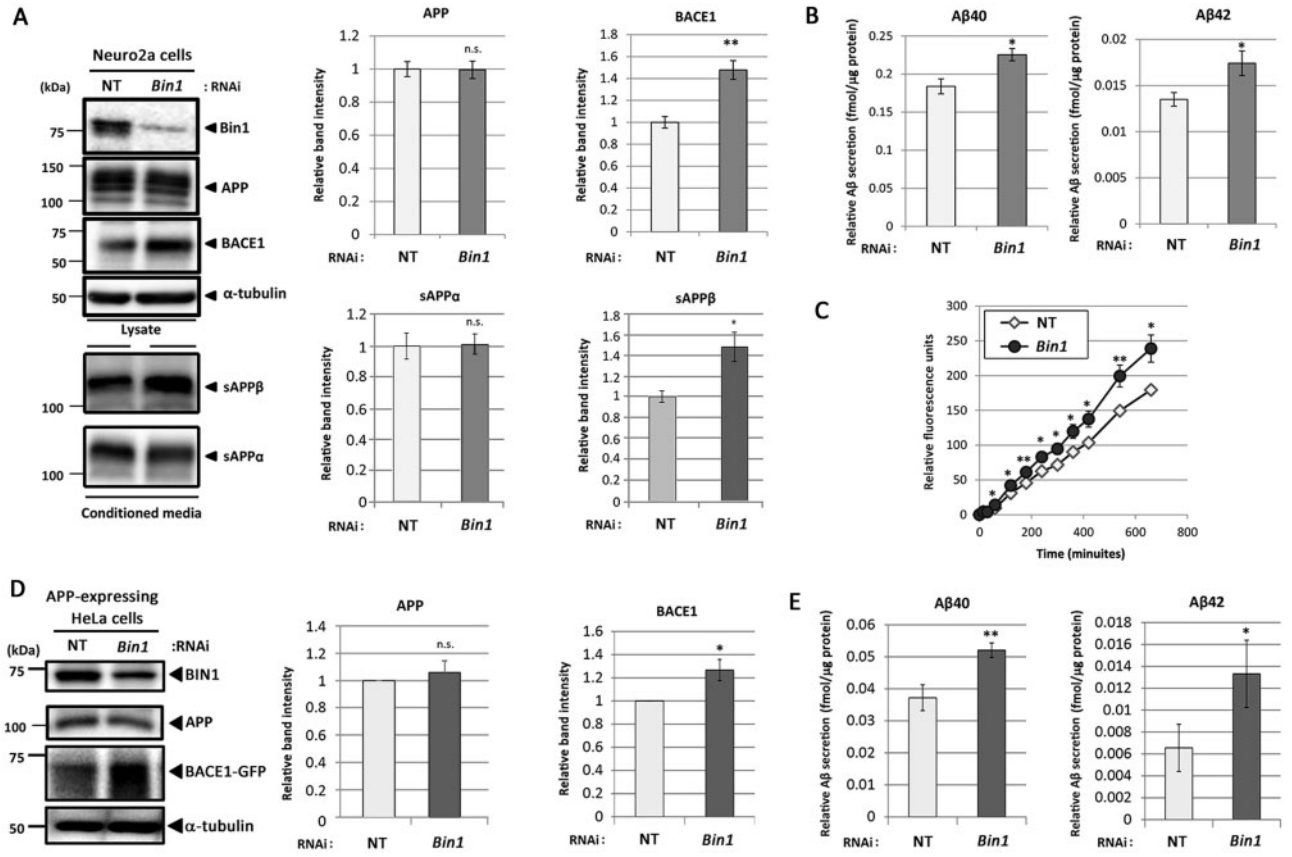


Figure 2. Depletion of BIN1 expression caused A$\beta$ overproduction with enhanced BACE1 activity. (**A**) Immnoblotting of the lysates and conditioned medium of Neuro2a cell transfected with a non-target (NT) or *Bin1* siRNA duplex. Relative band intensities are indicated at the right ($n = 6$, mean ± SEM, $^*P < 0.05$). (**B**) Levels of A$\beta$40 and A$\beta$42 secreted from dsRNA-transfected Neuro2a cells ($n = 6$, mean ± SEM, $^*P < 0.05$). (**C**) BACE1 activity in the membrane fractions of dsRNA-transfected Neuro2a cells was assessed by an *in vitro* assay ($n = 9$, mean ± SEM, $^*P < 0.05$, $^{**}P < 0.005$). (**D**) HeLa cells stably expressing BACE1-GFP were transfected with siRNA duplexes and a plasmid encoding APP. Relative band intensities of APP and BACE1-GFP are indicated at the right ($n = 5$, mean ± SEM, $^*P < 0.05$). (**E**) Levels of A$\beta$40 and A$\beta$42 secreted from HeLa cells expressing APP and BACE1-GFP, and transfected with a dsRNA against *Bin1* ($n = 7$, mean ± SEM, $^*P < 0.05$, $^{**}P < 0.005$).

the reduced degradation of BACE1. Ubiquitination at lysine 501 in the C-terminus of BACE1 is required for GGA3-mediated lysosomal targeting and the degradation of BACE1 (29,30). However, *Bin1* depletion increased the levels of BACE1 and Aβ secretion in the HeLa cells expressing the BACE1/K501R mutant (Fig. 4C and D), which cannot be ubiquitinated. Moreover, levels of ubiquitinated BACE1 was increased by *Bin1* RNAi (Fig. 4E), indicating that BACE1 was recruited and degraded by ubiquitin-dependent pathway in *Bin1*-depleted cells. These results indicated that the regulation of BACE1 trafficking and its degradation by BIN1 was an ubiquitin-independent, novel pathway of BACE1 metabolism.

### BAR domain of BIN1 is essential for its interaction with BACE1

To test the possibility that BIN1 directly recognizes with BACE1 as a cargo protein, we performed the *in vitro* GST-pulldown assay to examine the physical interaction between BIN1 and BACE1. We found that the GST-fused BACE1 C-terminal intracellular domain (B1CT) bound to the BIN1 holoprotein expressed in Neuro2a cells. As we used B1CT purified from bacterial lysates, these data support the notion that BIN1 recognizes the BACE1 intracellular domain without any post-translational modification including ubiquitination. To clarify which domain of BIN1 is responsible for its interaction with BACE1, we expressed BIN1 mutants lacking either the BAR domain (BIN1ΔBAR) or the SH3 domain (BIN1ΔSH3) (Fig. 5B) and performed pulldown assay. We found that the BAR domain, but not the SH3 domain of BIN1, was required for the binding of BIN1 with BACE1 (Fig. 5C). Furthermore, Neuro2a cells expressing BIN1ΔBAR showed increased level of BACE1 as well as Aβ secretion, similarly to that observed in *Bin1*-depleted cells (Fig. 6). Previous studies suggested that the SH3 domain of BIN1 is a molecular platform for the biogenesis of membrane tubules (31–33). In addition, the SH3 domain regulates the conformation of the BAR domain and its interaction with other molecules (34,35). Thus, the dominant-negative effect of the BIN1ΔBAR mutant might be due to the competition of the interaction between a limited amount of molecules involved in BIN1—BACE1 interaction and/or trafficking. These results indicated that the BAR domain of BIN1 recognizes the cytoplasmic domain of BACE1 to regulate the lysosomal targeting of BACE1 together with SH3 binding molecules, thereby affecting the production of Aβ.

## Discussion

Here we showed that the depletion of BIN1 increased the Aβ secretion by increasing cellular BACE1 levels. These results were observed both in neuronal and non-neuronal cells, indicating

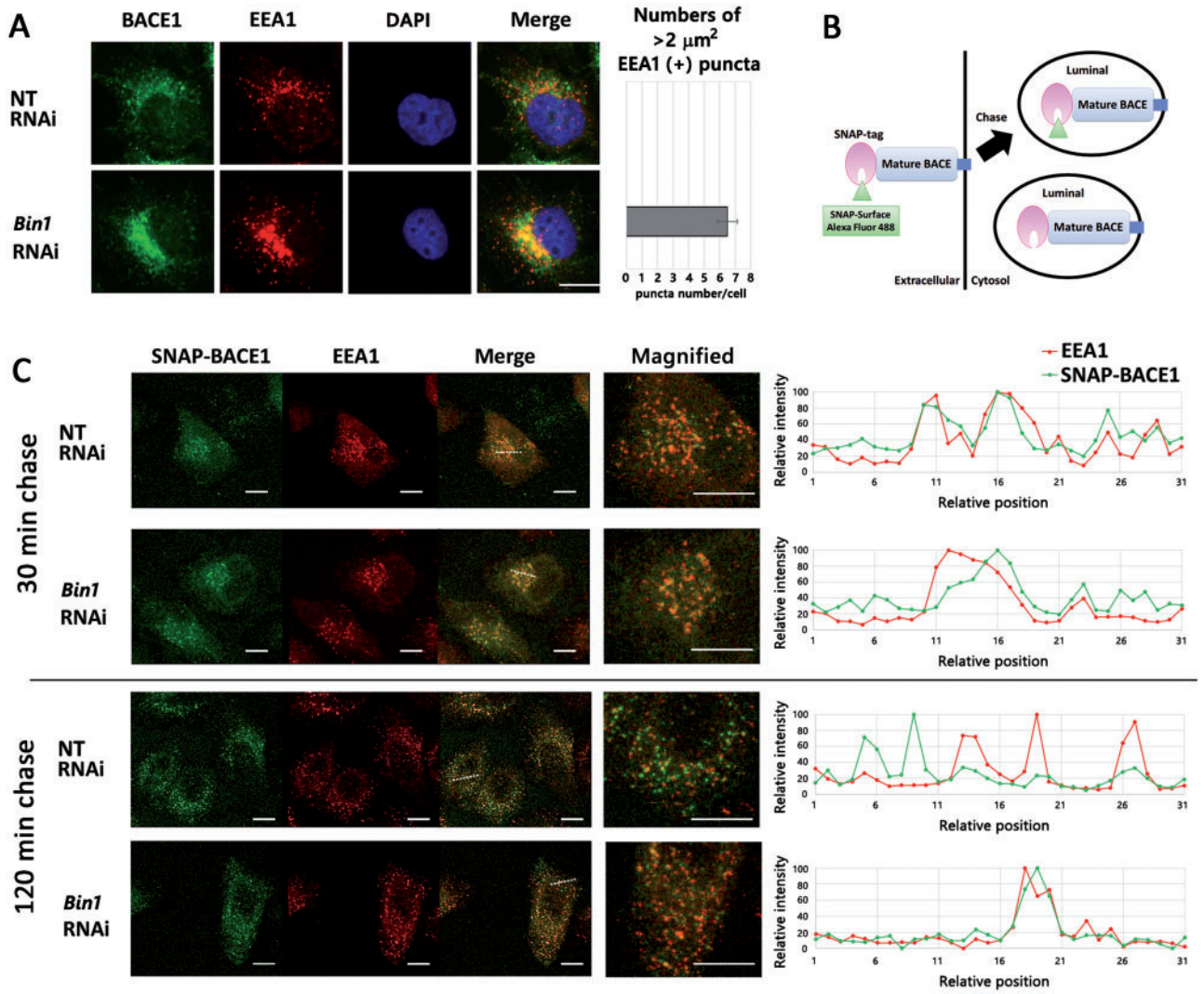


**Figure 3.** Depletion of BIN1 impaired the trafficking of intracellular BACE1 from early endosomes. (**A**) Immunocytochemical analysis of HeLa cells stably expressing BACE1-GFP treated with NT or *Bin1* RNAi using anti-GFP (green) and EEA1 (red) antibodies. Nuclei was visualized with DAPI (blue). Bar, 10 μm. Numbers of EEA1-positive puncta over 2 $\mu m^2$ per cell were indicated at the *right*. (**B**) Schematic depiction of the tracking of the intracellular transport of SNAP-BACE1 by specific cell surface labeling. (**C**) Uptake assay using SNAP-Surface Alexa Fluor 488 in HeLa cells expressing SNAP- BACE1 (green) treated with either NT or *Bin1* RNAi. After a 30 or 120 min chase, cells were fixed and stained with an anti-EEA1 antibody (red). Bar, 10 $\mu$m. A fluorescence intensity profiles along the dotted line in the merged image were shown in the *right* panel.

that the neuron-specific CLAP domain involved in clathrin-mediated endocytosis was not necessary for the regulation of BACE1 by BIN1. In fact, we found that the depletion of BIN1 caused the accumulation of BACE1 in the early endosomes where most of the β-cleavage of APP occurs, eventually leading to an increase in the production of Aβ. Consistent with this, cellular transferrin levels were increased in *Bin1* KO MEFs without an effect on transferrin internalization (18). In addition, the depletion of *Bin1* in HeLa cells impaired the recycling of transferrin, but not endocytosis, and cellular transferrin was accumulated in the juxtanuclear compartment (16). These data support our notion that the general function of BIN1 is regulation of the intracellular trafficking of cargos from the early endosome to the degradation pathway.

Understanding the precise role of BIN1 in BACE1 metabolism at the molecular level would provide a novel therapeutic target for AD in terms of targeting and modulating BACE1 cellular trafficking. We found that the BAR domain of BIN1 was a BACE1-interaction domain, although it still remains unclear as to whether BIN1 directly or indirectly associates with the cytoplasmic domain of BACE1. The BAR domain was initially implicated in the lipid binding of BIN1 and in sensing membrane curvature (11,36). However, the BAR domain is also known as a binding platform for several protein–protein interactions (37,38), suggesting that BACE1 is a novel cargo protein of BIN1 that is sorted from early endosomes to late endosomes/lysosomes. This is also consistent with a previous report that *Bin1* RNAi failed to affect Aβ production in HeLa cells expressing Swedish mutant APP (39), which is cleaved by BACE1 in early secretory compartments such as the *trans*-Golgi network (40). Intriguingly, ubiquitination at Lys-501 in the C-terminal intracellular domain of BACE1 was not required for its interaction with BIN1. The depletion of GGA3, which recognizes ubiquitinated BACE1, resulted in the reduced degradation of BACE1 in

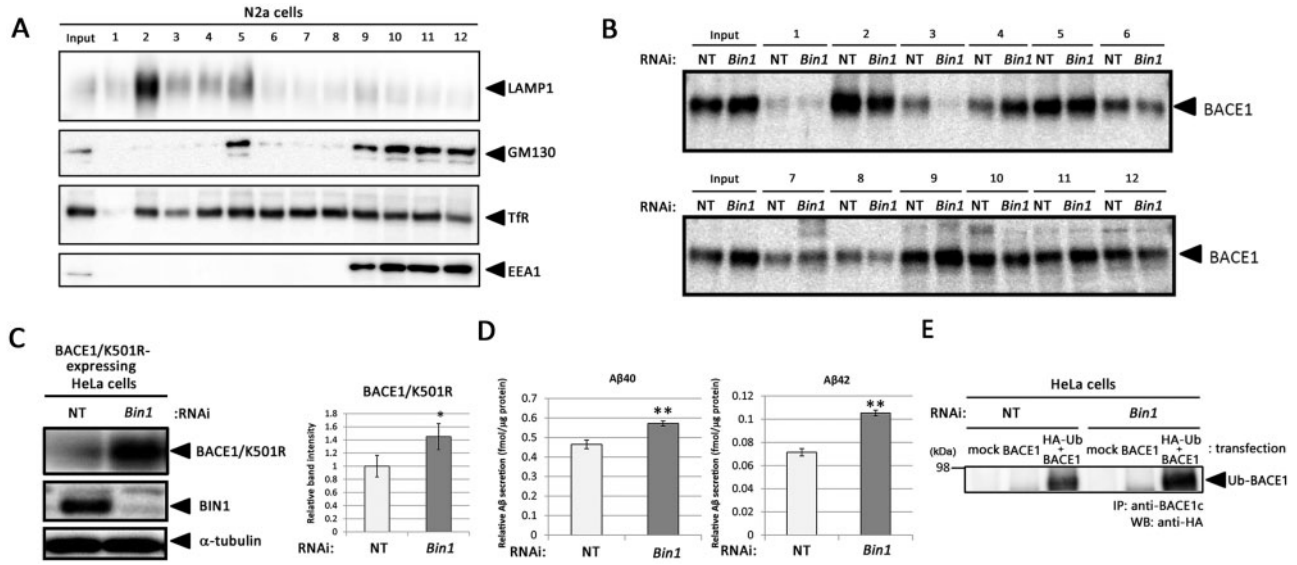


**Figure 4.** Depletion of BIN1 reduced the lysosomal targeting of BACE1.(**A**) Subcellular fractionation of the membranes of Neuro2a cells by sucrose density gradient centrifugation. Fractions 1–12 were taken from the top of the tube. LAMP1, GM130, TfR and EEA1 were used as a marker of late endosomes/lysosomes, the Golgi complex, recycling endosomes, and early endosomes, respectively. (**B**) Immunoblot analysis of fractions from Neuro2a cells transfected with NT or *Bin1* RNAi. Note that lysosomal localization (fraction 2) of BACE1 was decreased in *Bin1* depleted Neuro2a cells. (**C**) Immunoblot analysis of BACE1/K501R-expressing HeLa cells transfected with NT or *Bin1* RNAi. Levels of BACE1 were quantified at the right ($n = 4$, mean ± SEM, $^{*}P < 0.05$). (**D**) Levels of A$\beta$40 and A$\beta$42 secreted from BACE1/K501R-expressing HeLa cells transfected with dsRNA against *Bin1* ($n = 6$, mean ± SEM, $^{**}P < 0.005$). (**E**) Coimmunoprecipitation analysis of ubiquitinated BACE1 (Ub-BACE1) in the lysates from HeLa cells expressing HA-tagged ubiquitin and BACE1. Levels of immunoprecipitated Ub-BACE1 was increased in the BIN1 depleted HeLa cells.

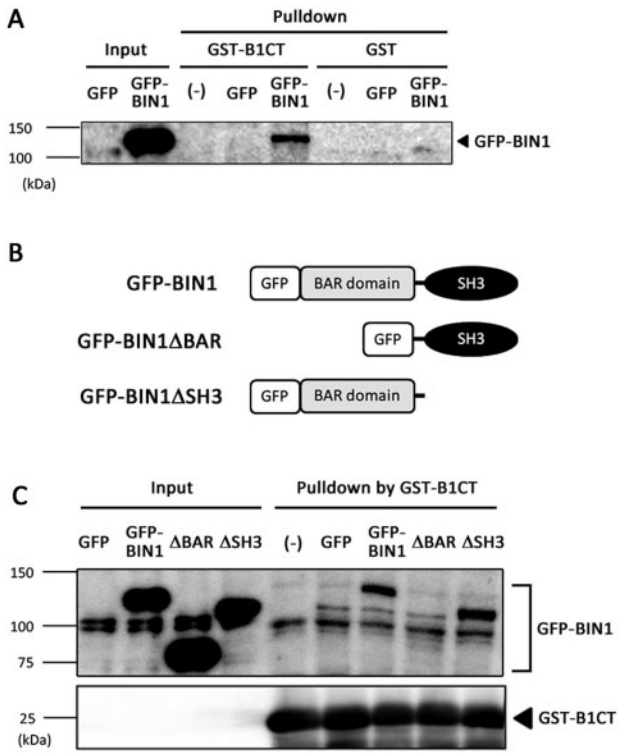


**Figure 5.** Binding of the BAR domain of BIN1 to the BACE1 C-terminal intracellular domain. (**A**) Immunoblot analysis of the pulldown fraction by GST or the GST- B1CT mixed with HeLa cell lysate expressing GFP or GFP-BIN1. (**B**) Schematic depiction of BIN1 mutants. (**C**) Immunoblot analysis of the pulldown fractions using HeLa cell lysates expressing GFP, GFP-BIN1, GFP-BIN1ΔBAR and GFP-BIN1ΔSH3.

the lysosomes and increased Aβ production in a similar manner to that observed in *Bin1*-depleted cells (30,41). Notably, we found that amount of ubiquitinated BACE1 was increased by *Bin1* RNAi (Fig. 4E). Thus, the level and activity of BACE1 is modulated by both ubiquitin-dependent and ubiquitin-independent trafficking, which are regulated by GGA3 and BIN1, respectively. We also found that the BIN1ΔBAR mutant showed dominant-negative effects. This suggests that a limited amount of partner proteins interacting with these domains is critical to BACE1 trafficking. It is noteworthy to mention that among the known BIN1-binding proteins, EHD family proteins play a role in the trafficking of internalized BACE1 in neurons (42). EHD proteins regulate BIN1 activity and are required for endocytic vesicle recycling together with Rab8a, Rab11-FIP2 and MICAL-L1 (16,43,44). Loss of EHD1 function compromised the recycling and axonal sorting of the internalized BACE1, thereby reducing Aβ production (42). Recently, the synaptic protein snapin, which is an EHD1-binding protein, was identified as a regulator of the endosome-to-lysosome retrograde transport of BACE1 (27,45). Snapin selectively recruits dynein motors to the BACE1-associated late endosomes. Thus, it will be interesting to test whether the functional associations between BIN1, EHD1 and snapin are involved in the regulation of the trafficking and/or the activity of BACE1 in neurons.

Our data suggested that a loss of BIN1 expression and/or function leads to the increased Aβ production and AD risk. However, whether the expression levels of BIN1 in AD patients were altered with polymorphism at rs6733839 is still controversial. Nevertheless, systematic analyses of BIN1 expression and alternative splicing patterns in AD patients in association with reported risk SNPs is required for understanding the molecular mechanism of how alterations of BIN1 function are involved in the pathogenesis of AD. In conclusion, we identified BIN1 as a novel genetic regulator of BACE1 intracellular trafficking and Aβ production. The BAR domain of BIN1 is essential for the

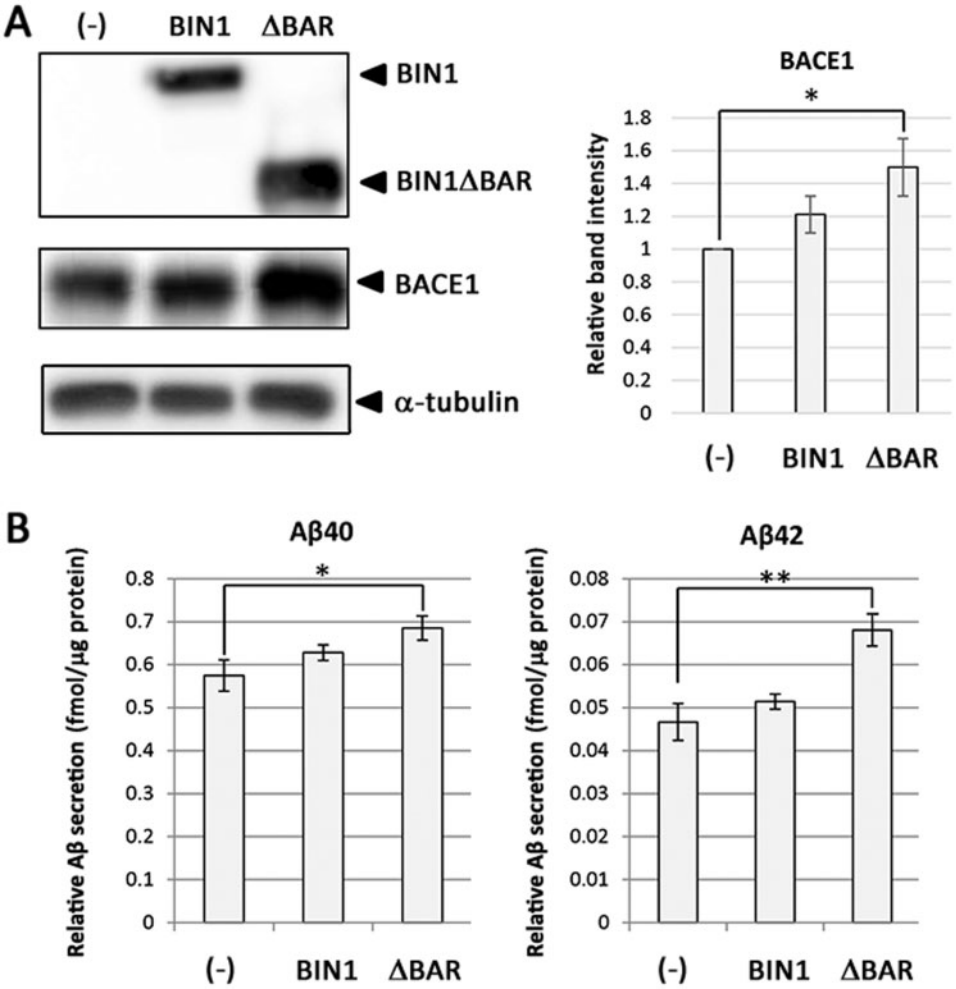


**Figure 6.** Deletion of the BAR domain of BIN1 caused increased A$\beta$ production and accumulation of BACE1. Immunoblot analysis of lysates from Neuro2a cells that were transfected with plasmids encoding mock ((−)), BIN1 or BIN1ΔBAR (ΔBAR). Levels of BACE1 are shown at the right ($n = 9$, mean ± SEM, $^*P < 0.05$). (**B**) Levels of A$\beta$40 and A$\beta$42 secreted from Neuro2a cells were quantified by sandwich ELISAs. ($n = 6$, mean ± SEM, $^*P < 0.05$, $^{**}P < 0.005$).

protein–protein interaction of BIN1 with BACE1. Further investigation of the molecular mechanism as to how the BAR domain interacts with the BACE1 intracellular domain, and whether BIN1 expression is misregulated in the AD patients are required for understanding the function of BIN1 in BACE1 intracellular trafficking and AD pathogenesis.

## Materials and Methods

### Molecular biology

The full length cDNA encoding human BIN1 isoform 1 (NCBI Reference Sequence: NM_139343.2) was amplified from a human fetal brain cDNA library using KOD plus neo DNA polymerase (TOYOBO). BIN1 mutants were generated by a standard mutagenesis protocol and subcloned into a pcDNA3.1 vector with a 3xmyc-tag sequence at the N-terminus [a kind gift from Dr Francis Barr (the University of Oxford)] or in a pEF5/FRT NF vector with an EGFP sequence at the N-terminus. Expression constructs encoding human BACE1 and full-length wild-type human $APP_{695}$ were subcloned into pEF6-V5 His TOPO TA or the pcDNA 3.1-hygro vector (Invitrogen) (22,46). Human BACE1 cDNA tagged with a SNAP tag at the N-terminus (SNAP-BACE1) or EGFP at the C-terminus (BACE1-GFP) were subcloned into the pcDNA 3.1-hygro vector and pEF6-V5 His TOPO TA vector, respectively. Bacterial expression constructs for recombinant Glutathione S transferase (GST) fusion proteins were generated from the pFAT2 vector encoding $His_6$-GST ($His_6$-GST/pFAT2). Lentiviral Cas9 vector was a gift from Drs. Eric Lander & David Sabatini (Addgene plasmid no. 50661) (47) and lentiviral gRNA vector was a gift from Dr Kosuke Yusa (Addgene plasmid no. 50947) (48). gRNA sequence for *Bace1* (5′-GATTCCTCGTCGGTCTCCCG-3′) was designed as previously described in (49). Expression plasmid for HA tagged ubiquitin was a kind gift from Dr Shigeo Murata (The University of Tokyo). The following Dharmacon ON-TARGET plus small interfering RNAs (Thermo Scientific) were used against human *Bin1* (no. J-008246-7) and mouse *Bin1* (no. L-054779-01). A non-targeting pool of siRNAs (no. D-001810-10) was used as a control.

### Antibodies and compounds

The following antibodies were commercially purchased: anti-BIN1 (clone 99D, Millipore; 1:400), anti-BACE1c (no. 18711, Immuno-Biological Laboratories; 1:250–1000), anti-APPc (no. 18961, Immuno-Biological Laboratories; 1:1000), anti-sAPPβ wild type (no. 18957, Immuno-Biological Laboratories; 1:250),

anti-βIII-tubulin TUJ1 (MAB1195, R&D Systems; 1:5000), anti-APP(597) (no. 28055, Immuno-Biological Laboratories; 1:1000), anti-α-tubulin DM1A (T6199, Sigma; 1:5000) anti-Nicastrin (N1660, SIGMA; 1:1000), anti-EEA1 (no. 610457, BD Biosciences; 1:200), anti-LAMP1 (CD107a, BD Biosciences; 1:500), anti-TGN46 (AHP500G, AbD Serotec; 1:250), anti- TfR (clone 236-15375, Invitrogen; 1:250), anti-HA high affinity (3F10, Roche Diagnostics; 1:1000), anti-DYKDDDDK tag (clone 1E6, WAKO Pure Chemical; 1:1000) and anti-GM130 (35/GM130, BD Biosciences; 1:1000). Specificity of anti-BACE1c antibody was confirmed by *Bace1* knockdown Neuro2a cells generated by CRISPR/Cas9 system (Supplemental Material Figure S2). The authentic BACE inhibitor (compound 16) was prepared according to the reported procedure (Supplemental Material, Figure S3A and B) (50). For preparation of (5-(prop-1-yn-1-yl)pyridin-3-yl) boronic acid from 3-bromo-5-(prop-1-yn-1-yl)pyridine, the procedure reported by Cai and coworkers was employed (51).

## Cell culture, transfection and RNA interference

Parental Neuro2a and HeLa S3 cells were cultured in Dulbecco's Modified Eagle Medium (DMEM) (Wako) containing 10% fetal bovine serum (FBS) (Hyclone), 50 U/ml penicillin and 50 mg/ml streptomycin (Invitrogen), at 37°C with 5% $CO_2$ (52,53). HeLa S3 cells stably expressing SNAP-BACE1 or BACE1-GFP were selected using 50 μg/ml blasticidin S and 200 μg/ml hygromycin, respectively. siRNAs at concentration of 20 nM were transfected using LipofectAMINE RNAiMAX (Invitrogen), or plasmids were transfected using Fugene 6 (Roche Applied Science) into cultured cells (20–30% confluence). Cells and media were harvested and analyzed 48–72 h after transfection. For CRIPSR/Cas9 system mediated genome editing, Neuro2a cells infected with recombinant lentivirus encoding humanized *S. pyogenes* Cas9 was selected by puromycin. FLAG-tagged Cas9 expression was induced by doxycycline. Stably Cas9-expressing monoclonal Neuro2a cell clone was screened by immunoblotting. Lentivirus encoding gRNA against *Bace1* was infected to the clonal culture, and the conditioned medium and cell lysates were harvested after 5 days of incubation with doxycycline-containing medium. Protein concentrations were measured using the BCA protein assay kit (Pierce). For immunoblot analysis, equal amounts of total protein (7.5–15 μg) per lane were separated on 7.5–12.5% Bis-Tris gels and transferred onto PVDF membranes. Band densities were analyzed using Image Quant LAS4000 (GE Healthcare). For analysis of Aβ secretion, the conditioned media were collected and subjected to sandwich-ELISAs using BNT77/BA27 and BNT77/BC05 for Aβ40 and Aβ42, respectively (53,54). Secreted Aβ was normalized by the concentration of the protein in the cell lysates.

## Immunocytochemical analysis

Cells were fixed for 15 min with 4% paraformaldehyde (PFA) and stained as previously described in (55). Fluorescence was visualized by a fluorescence microscope (AxioObserver Z1, Zeiss) with a ×40 Plan Apochromat oil immersion objective of NA 1.3 and AxioVision software, or a confocal microscope (SP5, Leica) with a ×63 PL APO CS oil-immersion objective of NA 1.4 and Leica LAS AF software. Image analyses including counting enlarged endosome and intensity analysis were processed using ImageJ software (NIH).

## *In vitro* BACE1 activity assay

Cell membranes of Neuro2a cells were used as the enzyme source (22). The BACE1-specific substrate JMV2236 (Bachem) in 25 mM $CH_3COONa$ (pH 4.5) was incubated at a final concentration of 10 μM at 37°C with the enzyme fraction in 1% CHAPSO detergent acidified by 25 mM $CH_3COONa$ (pH 4.5). Fluorescence was measured at an excitation wavelength of 320 nm and an emission wavelength of 420 nm. Specificity of this activity was confirmed by using 10 μM authentic BACE1 inhibitor (Supplementary Material Figure S3C).

## Ligand uptake assay

Subconfluent HeLa cells transfected with siRNAs and SNAP-BACE1 were incubated at 37°C in the DMEM containing 10% FBS. Media were replaced with fresh DMEM containing 5 μM SNAP Surface Alexa Fluor 488 (New England BioLabs) at 37°C for the indicated times. After incubation with SNAP Surface Alexa Fluor 488, cells were washed with PBS, and fixed with 4% PFA for immunocytochemical analysis. The contract and brightness are equally increased using Image J software.

## Protein expression, purification, and GST pull-down assay

The BACE1 intracellular domain tandemly fused with the His-tagged GST ($His_6$-GST/pFAT2) was expressed in *Escherichia coli* BL21 (DE3). GST fusion proteins were purified overnight using Ni-NTA agarose (Qiagen), and dialyzed with tris-buffered saline (50 mM Tris-HCl (pH 8.0), 150 mM NaCl) and stored at −80 °C. As the target protein, lysates from Neuro2a cells solubilized in lysis buffer containing 20 mM Tris-HCl (pH 7.6), 150 mM NaCl, 0.5% Triton X-100, Complete protease inhibitor cocktail (Roche) were precleared using glutathione sepharose (GE Healthcare) at 4°C for 1 h. For the GST pull-down assay, 1 mg of cleared cell lysates and 200 μg of GST fused proteins were mixed with lysis buffer containing 20 mM Tris-HCl (pH 7.6), 150 mM NaCl, 0.5% Triton X-100, Complete protease inhibitor cocktail, then incubated with 100 μl 50% glutathione sepharose beads on a rotator at 4°C for 90 min. Samples were eluted in sample buffer and analyzed by immunoblotting.

## Coimmunoprecipitation assay

After 24 h of siRNA transfection, expression vectors encoding BACE1 and HA tagged ubiquitin were transfected into HeLa cells. Cells were further incubated for 24 h and solubilized with RIPA buffer (50 mM Tris, 150mM NaCl, 1% NP-40, 1% Sodium deoxychlate, 0.1% SDS, pH7.5). Anti-BACE1c antibody (1:250 dilution) was added into RIPA soluble fraction obtained by centrifugation. After 24 h of incubation, 50 μl of protein G agarose (50% slurry) (GE Healthcare) was added into the samples and rotated 1 h. Immunoprecipitated materials were recovered by centrifugation and applied for immunoblot analysis.

## Quantitative RT-PCR

Total RNA from primary cortical neuron cultures was extracted using ISOGEN (Nippon Gene). ReverTra Ace qPCR RT Master Mix with gDNA remover (TOYOBO) was used to synthesize cDNA from the extracted RNA according to the manufacturer's instructions. Quantitative RT-PCR was performed using Light Cycler 480II (Roche) and THUNDERBIRD SYBR qPCR Mix

(TOYOBO) following the manufacturer's instructions. GAPDH was used as an internal control. Primers for BACE1 and GAPDH were as follows.

BACE1: 5′-GGAACCCATCTCGGCATCC-3′ and 5′-TCCGATTC CTCGTCGGTCTC-3′

GAPDH: 5′-AACGACCCCTTCATTGAC-3′ and 5′-GAAGACA CCAGTAGACTCCAC-3′

### Primary cortical neuron culture and lentivirus infection

Recombinant lentiviruses were produced using Lenti-X 293T cells (Takara) with three packaging plasmids (pCAG-kGP4.1R, pCAG4-RTR2 and pCAGGS-VSVG), which were a kind gift from Dr. Haruhiko Bito at the University of Tokyo (56). pFUGW plasmids encoding EGFP-NLS with or without Cre recombinase (EGFP-NLS-Cre or EGFP-NLS, respectively) under the ubiquitin promoter were used (57). Conditioned medium was collected as the second viral supernatant. These viral supernatants were concentrated using Lenti-X concentrator (Clontech). All experiments in the study using animals were performed in accordance with the guidelines for animal experiments provided by The University of Tokyo. All mice were maintained on food and water with a 12-h light/dark cycle. Primary cortical neurons were obtained from brains of P 1 pups, which were born from C57BL6J *Bin1*$^{flox/flox}$ female mice, for *in vitro* Cre-mediated *Bin1* ablation. Neurons were dissociated as previously described with some modifications (58,59). At days *in vitro* (DIV) 3, media were exchanged to non-viral Neurobasal medium containing 2 μM arabinofuranosyl cytosine (SIGMA). At DIV 4, media were changed to new Neurobasal medium without lentivirus or Ara-C, and incubated until DIV 10 and then harvested. Lysates and media were analyzed by immunoblotting and sandwich-ELISAs using BNT77/BA27 and BNT77/BC05 for Aβ40 and Aβ42, respectively.

### Sucrose density gradient fractionation

Isolation of lysosome-enriched fractions was performed as previously described with some modifications (60). Confluent Neuro2a cells cultured in 15-cm diameter dishes were harvested 60 h after the transfection of siRNAs. Cell pellets in homogenization buffer (20 mM HEPES pH 7.4, 150 mM $NaCl_2$, 2 mM $CaCl_2$, Complete protease inhibitor cocktail) were homogenized by passing through a 27-gauge needle eight times. The homogenates were centrifuged two times at 2500 rpm for 5 min at 4°C, and the post nuclear supernatants (PNS) were collected. PNS (0.9 ml) was mixed with 0.5 ml of 4 × homogenization buffer and 2 ml of 2 M sucrose to make a 40.6% sucrose fraction, and this fraction was loaded at the bottom of a centrifugation tube for the SW41 rotor (BECKMAN). To make the sucrose gradient, 4 ml of 35% sucrose in homogenization buffer was loaded onto the top of the 40.6% sucrose fraction, 3 ml of 25% sucrose in homogenization buffer was loaded onto the top of the 35% sucrose fraction, and 1 ml of homogenization buffer was loaded onto the top of the 25% sucrose fraction. Sucrose gradients were centrifuged using an SW41 rotor at 35 000 rpm for 90 min at 4°C. Five-hundred microliter of each fraction, from the top (fraction 1) to the bottom (fraction 12) were collected, and mixed with 400 μl of sterile distilled water, 100 μl of 0.15% Na-deoxycholate, and 140 μl of 100% trichloroacetic acid and incubated on ice for 1 h. After centrifugation at 14 000 rpm for 10 min at 4°C, the pellets were washed with pre-cooled acetone and centrifuged two times, and left at 37°C for 10 min to dry. The pellets were resuspended in sample buffer and analyzed by immunoblotting.

### Statistical analysis

Data were presented as mean values and error bars indicated SEMs. Groups were compared by the two-tailed Student's *t*-test. Significance was set at $^{*}P < 0.05$, and $^{**}P < 0.005$.

## Supplementary Material

Supplementary Material is available at *HMG* online.

## Acknowledgements

The authors are grateful to Takeda pharmaceutical company for providing Aβ ELISA, Dr Francis Barr (the University of Oxford), Dr Shigeo Murata and Dr Haruhiko Bito (the University of Tokyo) for constructs, Mr Ryota Ojima for technical assistance and our current and previous laboratory members for helpful discussions.

*Conflict of Interest statement*. None declared.

## Funding

This work was supported in part by Grants-in-Aid for Scientific Research (A) from the Japan Society for the Promotion of Science (15H02492 to T.T.), Scientific Research on Innovative Areas from the Ministry of Education, Culture, Sports, Science and Technology (26111705 to T.T.), by the Brain Mapping by Integrated Neurotechnologies for Disease Studies (Brain/MINDS) from the Japan Agency for Medical Research and Development (AMED) (14028022 and 15653129 to T.T.), the Platform Project for Supporting in Drug Discovery and Life Science Research (Platform for Drug Discovery, Informatics, and Structural Life Science) from AMED (to S.Y.), by Daiichi Sankyo Foundation of Life Science (to T.T.), by Ono Medical Research Foundation (to T.T.), and by NAGASE Science Technology Foundation (to T.T.).

## References

1. Hussain, I., Powell, D., Howlett, D.R., Tew, D.G., Meek, T.D., Chapman, C., Gloger, I.S., Murphy, K.E., Southan, C.D., Ryan, D.M. *et al.* (1999) Identification of a novel aspartic protease (Asp 2) as beta-secretase. *Mol. Cell. Neurosci.*, **14**, 419–427.
2. Sinha, S., Anderson, J.P., Barbour, R., Basi, G.S., Caccavello, R., Davis, D., Doan, M., Dovey, H.F., Frigon, N., Hong, J. *et al.* (1999) Purification and cloning of amyloid precursor protein beta-secretase from human brain. *Nature*, **402**, 537–540.
3. Vassar, R., Bennett, B.D., Babu-Khan, S., Kahn, S., Mendiaz, E.A., Denis, P., Teplow, D.B., Ross, S., Amarante, P., Loeloff, R. *et al.* (1999) Beta-secretase cleavage of Alzheimer's amyloid precursor protein by the transmembrane aspartic protease BACE. *Science*, **286**, 735–741.
4. Yan, R., Bienkowski, M.J., Shuck, M.E., Miao, H., Tory, M.C., Pauley, A.M., Brashier, J.R., Stratman, N.C., Mathews, W.R., Buhl, A.E. *et al.* (1999) Membrane-anchored aspartyl protease with Alzheimer's disease beta-secretase activity. *Nature*, **402**, 533–537.
5. Lin, X., Koelsch, G., Wu, S., Downs, D., Dashti, A. and Tang, J. (2000) Human aspartic protease memapsin 2 cleaves the beta-secretase site of beta-amyloid precursor protein. *Proc Natl Acad Sci U S A*, **97**, 1456–1460.

6. Zhang, X. and Song, W. (2013) The role of APP and BACE1 trafficking in APP processing and amyloid-beta generation. *Alzheimers Res. Ther.*, **5**, 46.
7. Sannerud, R., Declerck, I., Peric, A., Raemaekers, T., Menendez, G., Zhou, L., Veerle, B., Coen, K., Munck, S., De Strooper, B. *et al.* (2011) ADP ribosylation factor 6 (ARF6) controls amyloid precursor protein (APP) processing by mediating the endosomal sorting of BACE1. *Proc. Natl. Acad. Sci. USA*, **108**, E559–E568.
8. Morohashi, Y. and Tomita, T. (2013) Protein trafficking and maturation regulate intramembrane proteolysis. *Biochim. Biophys. Acta*, **1828**, 2855–2861.
9. Tan, M.S., Yu, J.T. and Tan, L. (2013) Bridging integrator 1 (BIN1): form, function, and Alzheimer's disease. *Trends Mol. Med.*, **19**, 594–603.
10. Lambert, J.C., Ibrahim-Verbaas, C.A., Harold, D., Naj, A.C., Sims, R., Bellenguez, C., DeStafano, A.L., Bis, J.C., Beecham, G.W., Grenier-Boley, B. *et al.* (2013) Meta-analysis of 74,046 individuals identifies 11 new susceptibility loci for Alzheimer's disease. *Nat. Genet.*, **45**, 1452–1458.
11. Prokic, I., Cowling, B.S. and Laporte, J. (2014) Amphiphysin 2 (BIN1) in physiology and diseases. *J. Mol. Med. (Berl)*, **92**, 453–463.
12. Lee, E., Marcucci, M., Daniell, L., Pypaert, M., Weisz, O.A., Ochoa, G.C., Farsad, K., Wenk, M.R. and De Camilli, P. (2002) Amphiphysin 2 (Bin1) and T-tubule biogenesis in muscle. *Science*, **297**, 1193–1196.
13. Butler, M.H., David, C., Ochoa, G.C., Freyberg, Z., Daniell, L., Grabs, D., Cremona, O. and De Camilli, P. (1997) Amphiphysin II (SH3P9; BIN1), a member of the amphiphysin/Rvs family, is concentrated in the cortical cytomatrix of axon initial segments and nodes of ranvier in brain and around T tubules in skeletal muscle. *J. Cell. Biol.*, **137**, 1355–1367.
14. Wechsler-Reya, R.J., Elliott, K.J. and Prendergast, G.C. (1998) A role for the putative tumor suppressor Bin1 in muscle cell differentiation. *Mol. Cell. Biol.*, **18**, 566–575.
15. Leprince, C., Le Scolan, E., Meunier, B., Fraisier, V., Brandon, N., De Gunzburg, J. and Camonis, J. (2003) Sorting nexin 4 and amphiphysin 2, a new partnership between endocytosis and intracellular trafficking. *J. Cell. Sci.*, **116**, 1937–1948.
16. Pant, S., Sharma, M., Patel, K., Caplan, S., Carr, C.M. and Grant, B.D. (2009) AMPH-1/Amphiphysin/Bin1 functions with RME-1/Ehd1 in endocytic recycling. *Nat. Cell. Biol.*, **11**, 1399–1410.
17. Chapuis, J., Hansmannel, F., Gistelinck, M., Mounier, A., Van Cauwenberghe, C., Kolen, K.V., Geller, F., Sottejeau, Y., Harold, D., Dourlen, P. *et al.* (2013) Increased expression of BIN1 mediates Alzheimer genetic risk by modulating tau pathology. *Mol. Psychiatry*, **18**, 1225–1234.
18. Muller, A.J., Baker, J.F., DuHadaway, J.B., Ge, K., Farmer, G., Donover, P.S., Meade, R., Reid, C., Grzanna, R., Roach, A.H. *et al.* (2003) Targeted disruption of the murine Bin1/Amphiphysin II gene does not disable endocytosis but results in embryonic cardiomyopathy with aberrant myofibril formation. *Mol. Cell. Biol.*, **23**, 4295–4306.
19. Chang, M.Y., Boulden, J., Sutanto-Ward, E., Duhadaway, J.B., Soler, A.P., Muller, A.J. and Prendergast, G.C. (2007) Bin1 ablation in mammary gland delays tissue remodeling and drives cancer progression. *Cancer Res.*, **67**, 100–107.
20. Wechsler-Reya, R., Sakamuro, D., Zhang, J., Duhadaway, J. and Prendergast, G.C. (1997) Structural analysis of the human BIN1 gene. Evidence for tissue-specific transcriptional regulation and alternate RNA splicing. *J. Biol. Chem.*, **272**, 31453–31458.
21. Ge, K., DuHadaway, J., Du, W., Herlyn, M., Rodeck, U. and Prendergast, G.C. (1999) Mechanism for elimination of a tumor suppressor: aberrant splicing of a brain-specific exon causes loss of function of Bin1 in melanoma. *Proc. Natl. Acad. Sci. USA*, **96**, 9689–9694.
22. Takasugi, N., Sasaki, T., Suzuki, K., Osawa, S., Isshiki, H., Hori, Y., Shimada, N., Higo, T., Yokoshima, S., Fukuyama, T. *et al.* (2011) BACE1 activity is modulated by cell-associated sphingosine-1-phosphate. *J. Neurosci.*, **31**, 6850–6857.
23. Prendergast, G.C., Muller, A.J., Ramalingam, A. and Chang, M.Y. (2009) BAR the door: cancer suppression by amphiphysin-like genes. *Biochim. Biophys. Acta*, **1795**, 25–36.
24. Maurel, D., Comps-Agrar, L., Brock, C., Rives, M.L., Bourrier, E., Ayoub, M.A., Bazin, H., Tinel, N., Durroux, T., Prezeau, L. *et al.* (2008) Cell-surface protein-protein interaction analysis with time-resolved FRET and snap-tag technologies: application to GPCR oligomerization. *Nat. Methods*, **5**, 561–567.
25. Keppler, A., Gendreizig, S., Gronemeyer, T., Pick, H., Vogel, H. and Johnsson, K. (2003) A general method for the covalent labeling of fusion proteins with small molecules in vivo. *Nat. Biotechnol.*, **21**, 86–89.
26. Koh, Y.H., von Arnim, C.A., Hyman, B.T., Tanzi, R.E. and Tesco, G. (2005) BACE is degraded via the lysosomal pathway. *J. Biol. Chem.*, **280**, 32499–32504.
27. Ye, X. and Cai, Q. (2014) Snapin-mediated BACE1 retrograde transport is essential for its degradation in lysosomes and regulation of APP processing in neurons. *Cell Rep.*, **6**, 24–31.
28. Kizuka, Y., Kitazume, S., Fujinawa, R., Saito, T., Iwata, N., Saido, T.C., Nakano, M., Yamaguchi, Y., Hashimoto, Y., Staufenbiel, M. *et al.* (2015) An aberrant sugar modification of BACE1 blocks its lysosomal targeting in Alzheimer's disease. *EMBO Mol. Med.*, **7**, 175–189.
29. Kang, E.L., Biscaro, B., Piazza, F. and Tesco, G. (2012) BACE1 protein endocytosis and trafficking are differentially regulated by ubiquitination at lysine 501 and the Di-leucine motif in the carboxyl terminus. *J. Biol. Chem.*, **287**, 42867–42880.
30. Kang, E.L., Cameron, A.N., Piazza, F., Walker, K.R. and Tesco, G. (2010) Ubiquitin regulates GGA3-mediated degradation of BACE1. *J. Biol. Chem.*, **285**, 24108–24119.
31. Nicot, A.S., Toussaint, A., Tosch, V., Kretz, C., Wallgren-Pettersson, C., Iwarsson, E., Kingston, H., Garnier, J.M., Biancalana, V., Oldfors, A. *et al.* (2007) Mutations in amphiphysin 2 (BIN1) disrupt interaction with dynamin 2 and cause autosomal recessive centronuclear myopathy. *Nat. Genet.*, **39**, 1134–1139.
32. Falcone, S., Roman, W., Hnia, K., Gache, V., Didier, N., Laine, J., Aurade, F., Marty, I., Nishino, I., Charlet-Berguerand, N. *et al.* (2014) N-WASP is required for Amphiphysin-2/BIN1-dependent nuclear positioning and triad organization in skeletal muscle and is involved in the pathophysiology of centronuclear myopathy. *EMBO Mol. Med.*, **6**, 1455–1475.
33. Royer, B., Hnia, K., Gavriilidis, C., Tronchere, H., Tosch, V. and Laporte, J. (2013) The myotubularin-amphiphysin 2 complex in membrane tubulation and centronuclear myopathies. *EMBO Rep.*, **14**, 907–915.
34. Wu, T. and Baumgart, T. (2014) BIN1 membrane curvature sensing and generation show autoinhibition regulated by downstream ligands and PI(4,5)P2. *Biochemistry*, **53**, 7297–7309.
35. Meinecke, M., Boucrot, E., Camdere, G., Hon, W.C., Mittal, R. and McMahon, H.T. (2013) Cooperative recruitment of dynamin and BIN/amphiphysin/Rvs (BAR) domain-containing

proteins leads to GTP-dependent membrane scission. *J. Biol. Chem.*, **288**, 6651–6661.
36. Casal, E., Federici, L., Zhang, W., Fernandez-Recio, J., Priego, E.M., Miguel, R.N., DuHadaway, J.B., Prendergast, G.C., Luisi, B.F. and Laue, E.D. (2006) The crystal structure of the BAR domain from human Bin1/amphiphysin II and its implications for molecular recognition. *Biochemistry*, **45**, 12917–12928.
37. Habermann, B. (2004) The BAR-domain family of proteins: a case of bending and binding? *EMBO Rep.*, **5**, 250–255.
38. Ramalingam, A., Farmer, G.E., Stamato, T.D. and Prendergast, G.C. (2007) Bin1 interacts with and restrains the DNA end-binding protein complex Ku. *Cell Cycle*, **6**, 1914–1918.
39. Bali, J., Gheinani, A.H., Zurbriggen, S. and Rajendran, L. (2012) Role of genes linked to sporadic Alzheimer's disease risk in the production of beta-amyloid peptides. *Proc. Natl. Acad. Sci. USA*, **109**, 15307–15311.
40. Thinakaran, G., Teplow, D.B., Siman, R., Greenberg, B. and Sisodia, S.S. (1996) Metabolism of the "Swedish" amyloid precursor protein variant in neuro2a (N2a) cells. Evidence that cleavage at the "beta-secretase" site occurs in the golgi apparatus. *J Biol Chem*, **271**, 9390–9397.
41. Walker, K.R., Kang, E.L., Whalen, M.J., Shen, Y. and Tesco, G. (2012) Depletion of GGA1 and GGA3 mediates postinjury elevation of BACE1. *J. Neurosci.*, **32**, 10423–10437.
42. Buggia-Prevot, V., Fernandez, C.G., Udayar, V., Vetrivel, K.S., Elie, A., Roseman, J., Sasse, V.A., Lefkow, M., Meckler, X., Bhattacharyya, S. *et al.* (2013) A function for EHD family proteins in unidirectional retrograde dendritic transport of BACE1 and Alzheimer's disease Abeta production. *Cell Rep.*, **5**, 1552–1563.
43. Naslavsky, N. and Caplan, S. (2011) EHD proteins: key conductors of endocytic transport. *Trends Cell. Biol.*, **21**, 122–131.
44. Posey, A.D., Jr., Swanson, K.E., Alvarez, M.G., Krishnan, S., Earley, J.U., Band, H., Pytel, P., McNally, E.M. and Demonbreun, A.R. (2014) EHD1 mediates vesicle trafficking required for normal muscle growth and transverse tubule development. *Dev. Biol.*, **387**, 179–190.
45. Wei, S., Xu, Y., Shi, H., Wong, S.H., Han, W., Talbot, K., Hong, W. and Ong, W.Y. (2010) EHD1 is a synaptic protein that modulates exocytosis through binding to snapin. *Mol. Cell. Neurosci.*, **45**, 418–429.
46. Iwata, H., Tomita, T., Maruyama, K. and Iwatsubo, T. (2001) Subcellular compartment and molecular subdomain of beta-amyloid precursor protein relevant to the Abeta 42-promoting effects of Alzheimer mutant presenilin 2. *J. Biol. Chem.*, **276**, 21678–21685.
47. Wang, T., Wei, J.J., Sabatini, D.M. and Lander, E.S. (2014) Genetic screens in human cells using the CRISPR-Cas9 system. *Science*, **343**, 80–84.
48. Koike-Yusa, H., Li, Y., Tan, E.P., Velasco-Herrera Mdel, C. and Yusa, K. (2014) Genome-wide recessive genetic screening in mammalian cells with a lentiviral CRISPR-guide RNA library. *Nat. Biotechnol.*, **32**, 267–273.
49. Ran, F.A., Hsu, P.D., Wright, J., Agarwala, V., Scott, D.A. and Zhang, F. (2013) Genome engineering using the CRISPR-Cas9 system. *Nat. Protoc.*, **8**, 2281–2308.
50. Stamford, A.W., Scott, J.D., Li, S.W., Babu, S., Tadesse, D., Hunter, R., Wu, Y., Misiaszek, J., Cumming, J.N., Gilbert, E.J. *et al.* (2012) Discovery of an Orally Available, Brain Penetrant BACE1 Inhibitor that Affords Robust CNS Abeta Reduction. *ACS Med. Chem. Lett.*, **3**, 897–902.
51. Cai, D., Larsen, R.D. and Reider, P.J. (2002) Effective lithiation of 3-bromopyridine: synthesis of 3-pyridine boronic acid and variously 3-substituted pyridines. *Tetrahedron Lett.*, **43**, 4285–4287.
52. Morohashi, Y., Kan, T., Tominari, Y., Fuwa, H., Okamura, Y., Watanabe, N., Sato, C., Natsugari, H., Fukuyama, T., Iwatsubo, T. *et al.* (2006) C-terminal fragment of presenilin is the molecular target of a dipeptidic gamma-secretase-specific inhibitor DAPT (N-[N-(3,5-difluorophenacetyl)-L-alanyl]-S-phenylglycine t-butyl ester). *J. Biol. Chem.*, **281**, 14670–14676.
53. Tomita, T., Maruyama, K., Saido, T.C., Kume, H., Shinozaki, K., Tokuhiro, S., Capell, A., Walter, J., Grunberg, J., Haass, C. *et al.* (1997) The presenilin 2 mutation (N141I) linked to familial Alzheimer disease (Volga German families) increases the secretion of amyloid beta protein ending at the 42nd (or 43rd) residue. *Proc. Natl. Acad. Sci. USA*, **94**, 2025–2030.
54. Asami-Odaka, A., Ishibashi, Y., Kikuchi, T., Kitada, C. and Suzuki, N. (1995) Long amyloid beta-protein secreted from wild-type human neuroblastoma IMR-32 cells. *Biochemistry*, **34**, 10272–10278.
55. Kanatsu, K., Morohashi, Y., Suzuki, M., Kuroda, H., Watanabe, T., Tomita, T. and Iwatsubo, T. (2014) Decreased CALM expression reduces Abeta42 to total Abeta ratio through clathrin-mediated endocytosis of gamma-secretase. *Nat. Commun.*, **5**, 3386.
56. Okuno, H., Akashi, K., Ishii, Y., Yagishita-Kyo, N., Suzuki, K., Nonaka, M., Kawashima, T., Fujii, H., Takemoto-Kimura, S., Abe, M. *et al.* (2012) Inverse synaptic tagging of inactive synapses via dynamic interaction of Arc/Arg3.1 with CaMKIIbeta. *Cell*, **149**, 886–898.
57. Ho, A., Morishita, W., Atasoy, D., Liu, X., Tabuchi, K., Hammer, R.E., Malenka, R.C. and Sudhof, T.C. (2006) Genetic analysis of Mint/X11 proteins: essential presynaptic functions of a neuronal adaptor protein family. *J. Neurosci.*, **26**, 13089–13101.
58. Suzuki, K., Hayashi, Y., Nakahara, S., Kumazaki, H., Prox, J., Horiuchi, K., Zeng, M., Tanimura, S., Nishiyama, Y., Osawa, S. *et al.* (2012) Activity-dependent proteolytic cleavage of neuroligin-1. *Neuron*, **76**, 410–422.
59. Fukumoto, H., Tomita, T., Matsunaga, H., Ishibashi, Y., Saido, T.C. and Iwatsubo, T. (1999) Primary cultures of neuronal and non-neuronal rat brain cells secrete similar proportions of amyloid beta peptides ending at A beta40 and A beta42. *Neuroreport*, **10**, 2965–2969.
60. Raben, N., Shea, L., Hill, V. and Plotz, P. (2009) Monitoring autophagy in lysosomal storage disorders. *Methods Enzymol.*, **453**, 417–449.